

Vertical single- and double-walled carbon nanotubes grown from modified porous anodic alumina templates

Matthew R Maschmann^{1,2}, Aaron D Franklin^{1,3},
Placidus B Amama¹, Dmitri N Zakharov¹, Eric A Stach^{1,4},
Timothy D Sands^{1,3,4} and Timothy S Fisher^{1,2,5}

¹ Birck Nanotechnology Center, Purdue University, West Lafayette, IN 47907, USA

² School of Mechanical Engineering, Purdue University, West Lafayette, IN 47907, USA

³ School of Electrical and Computer Engineering, Purdue University, West Lafayette, IN 47907, USA

⁴ School of Materials Engineering, Purdue University, West Lafayette, IN 47907, USA

E-mail: tsfisher@purdue.edu

Received 24 April 2006, in final form 20 June 2006

Published 11 July 2006

Online at stacks.iop.org/Nano/17/3925

Abstract

Vertical single-walled and double-walled carbon nanotube (SWNT and DWNT) arrays have been grown using a catalyst embedded within the pore walls of a porous anodic alumina (PAA) template. The initial film structure consisted of a SiO_x adhesion layer, a Ti layer, a bottom Al layer, a Fe layer, and a top Al layer deposited on a Si wafer. The Al and Fe layers were subsequently anodized to create a vertically oriented pore structure through the film stack. CNTs were synthesized from the catalyst layer by plasma-enhanced chemical vapour deposition (PECVD). The resulting structure is expected to form the basis for development of vertically oriented CNT-based electronics and sensors.

1. Introduction

Single-walled and double-walled carbon nanotubes (SWNTs and DWNTs) have been extensively studied for use in electronic devices because of their desirable electronic transport properties and potential for high-density integration [1–4]. Numerous simple CNT-based electronic devices have been reported [4–8], but all have incorporated CNTs synthesized or dispersed in a horizontal direction, parallel to the substrate. More densely packed structures may be realized by orienting nanotubes in the vertical direction, perpendicular to the substrate. One possible method for controlled vertical synthesis is the use of a nanoporous template, such as porous anodic alumina (PAA), which acts as a spatial constraint and allows growth to proceed through a narrow vertical channel.

To our knowledge, direct SWNT and DWNT synthesis from within a PAA template has not yet been reported. PAA templates have been used in the synthesis of vertically oriented

multi-walled CNTs (MWNTs) [9–13] and MWNT devices [14] that take the diameter of the PAA pore walls [15, 16] from which they originate—typically 30–50 nm. These synthesis methods proceed using a catalyst metal electrodeposited into the bottom of pores [9–14, 16] or by direct carbon deposition on the template wall, using no metal catalyst [15]. However, these large-diameter MWNTs do not exploit the enhanced electronic transport afforded by the unique electrical properties of SWNTs and DWNTs and are typically greater than an order of magnitude larger in diameter.

We report the synthesis of SWNTs and DWNTs from within an ordered nanoporous alumina template that could form the basis for vertically oriented SWNT and DWNT CNT electronic and sensing devices. The template is similar to that of PAA, with the addition of a CNT catalyst metal embedded directly into the PAA film structure, as shown in figure 1. CNT synthesis occurs in a microwave PECVD system that has been shown to enhance the vertical alignment of SWNTs for other catalytic systems [17]. Because CNT synthesis in the modified PAA structure is initiated in a spatially confined

⁵ Author to whom any correspondence should be addressed.

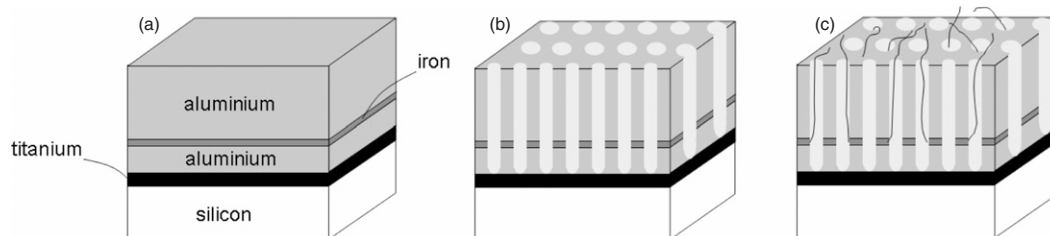


Figure 1. Schematic diagram of catalyst preparation and CNT synthesis procedure. (a) Initial deposited film structure. (b) Anodized film structure. (c) CNTs synthesized from pore channels.

pore, nanotubes emerging from the pores must be vertically aligned within the pore channel. A Ti layer beneath the PAA pore structure is intended to serve as an electrode for subsequent electrodeposition of metallic contacts to address the bottom surface of CNTs for device integration. Because the diameter of the SWNTs and DWNTs growing from the structure are negligible compared to the pore diameter in which they grow, functionalization of the CNTs by addition of a gate dielectric material or biological agent may proceed within the vertical channel, allowing for a functional device to be entirely confined in individual pores.

2. Experimental details

Ordered nanoporous films were synthesized using a procedure similar to that for standard PAA films [10, 11, 13]. Several thin films were deposited on silicon substrates using electron beam evaporation at a base pressure of 5×10^{-7} Torr. First, a SiO_x film of 50 nm was deposited on the substrate to promote adhesion of subsequent layers. Titanium was then deposited to a thickness of 150 nm to act as an electrically conductive layer for future electrodeposition of contact metal after nanotube synthesis. A 100–200 nm bottom layer of Al was then deposited on the Ti layer, followed by a layer of Fe ranging in thickness from 0.5 to 20 nm. A top Al layer several hundred nanometres to one micron thick was then deposited to complete the film. A schematic diagram of the film structure and the synthesis procedure is shown in figure 1.

The top layers of Al and Fe were anodized to the Ti layer using a double-anodization procedure [18] to control the final thickness of the top Al layer. Oxalic acid (0.3 M) and sulfuric acid (0.3 M) at 4 °C were used as the working electrolytes, with anodization potentials ranging from 40 to 80 V using oxalic acid and 20 V when using sulfuric acid. If larger diameter pores were desired after anodization, the sample was immersed in a 0.1 M H_3PO_4 solution to widen the pores (see figure 2(d)). Proper choice of anodization electrolyte and potential allows for optimization of pore size and pitch for a given application. A Pt mesh screen served as the cathode. Anodization of the Al layers proceeded with a nominal current density of 2 mA cm^{-2} ; however, a sharp increase in current density of up to 250 mA cm^{-2} was observed while anodizing through the Fe layer, with vigorous bubble production observed. When the current density decreased to a negligible value upon completion of anodization, as observed in previous reports [19], anodization

was immediately terminated. Rabin *et al* [19], Tian *et al* [20], and Franklin *et al* [21] have shown that anodization of Al films supported on a Ti layer does not fully oxidize the Ti, and electrodeposition of metallic nanowires using the bottom Ti layer as an electrode was possible. A similar technique could be incorporated with this structure to electrically address the CNTs.

After anodization of the catalytic film, ordered pores with diameters of 20–50 nm were observed (see figure 2), depending on the anodization conditions. Cross-sectional FESEM images reveal a disruption in the vertical order of some pores at the Fe layer, as seen in figures 2(a) and (c); however, anodization continued through the Fe and bottom Al layers, ceasing at the bottom Ti layer. The catalyst metal was thereby locally embedded into the pore wall structure, allowing for exposure to reactive gases during synthesis. It is believed that alumina surrounds the catalyst particles [22–26], impeding aggregation of the catalyst and enabling retention of catalytic activity for SWNT and DWNT synthesis. Fe was found to be most compatible for integration into the PAA structure, as it was significantly more catalytically active than Ni, Co, and Pd and did not lead to film delamination during anodization.

CNT synthesis was conducted using a microwave plasma-enhanced chemical vapour deposition (PECVD) reactor [27]. During synthesis, the substrate's top surface temperature was measured by a Williamson (model 90) dual wavelength pyrometer aimed at the centre of the test substrate, while a K-type thermocouple embedded in the graphite susceptor stage measured stage temperature. Standard synthesis conditions include 300 W microwave plasma power, 10 Torr pressure, 50 sccm hydrogen, 10 sccm methane, 900 °C stage temperature for 10 min. The substrate surface temperature ranged from 770 to 800 °C during syntheses. After synthesis, the chamber was immediately evacuated to remove reactive species, and the sample was allowed to cool to room temperature before being removed from the chamber.

A Hitachi S-4800 cold field emission scanning electron microscope (FESEM) was utilized for SEM imaging. High-resolution transmission electron microscopy (HRTEM) was carried out on an FEI Titan 80/300 field emission electron microscope with a point-to-point resolution of 2 Å at 300 kV. Samples for TEM were prepared by CNTs dispersion from the template using a sonication in ethanol for 30 min followed by centrifugation for 10 min. Afterwards a drop of the dispersed solution was placed on a lacey carbon TEM copper grid to allow imaging of individual CNTs.

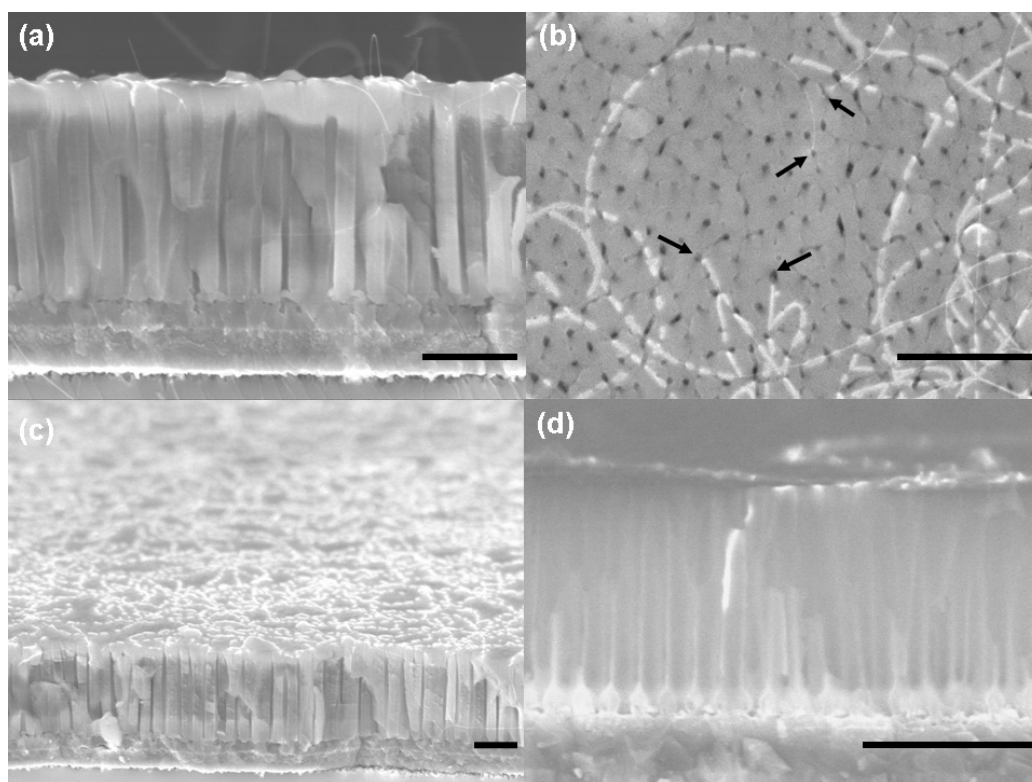


Figure 2. FESEM images of nanoporous alumina template and CNTs. (a) Cross-sectional view showing vertical alignment of some CNTs. (b) Top PAA surface showing CNTs emerging from pores. (c) Tilted cross-sectional view of template and CNTs. (d) Cross-sectional view showing CNT initiating from catalyst layer. The deposited film structure was (SiO_x/Ti/Al/Fe/Al) 50/150/100/2/700 nm for (a)–(c) and 50/150/200/3/500 for (d). Samples (a) and (c) were anodized in 0.3 M oxalic acid at 80 V, while (b) and (d) were anodized at 40 V. Sample (d) underwent 0.1 M H₃PO₄ pore widening. Scale bar = 500 nm.

3. Results and discussion

Small-diameter CNTs can be observed within the pore structure after PECVD synthesis using FESEM imaging, as shown in figure 2. Lengths of the CNTs exceed several microns, and bundles consisting of many CNTs are observed merging on the PAA surface. The localized high-contrast signatures produced when CNTs contacted the top alumina surface due to electron beam charging effects was advantageous for locating the CNTs by FESEM but made diameter estimations difficult. Quantification of CNT population density from PAA pores using FESEM imaging is inherently difficult but is further complicated by the many orientations of CNTs with respect to the focal plane (figures 2(a)–(c)). Additionally, the formation of bundles consisting of many CNTs further complicates locating the pore of origin of individual SWNTs. We estimate that approximately 10% of pores generate CNTs for the film configurations producing the highest density, and only one CNT is observed emerging for each catalytically active pore. Further optimization of film structure, anodization, and synthesis conditions are expected to increase CNT density.

Many of the CNTs emerging from the top PAA surface are vertically oriented, as seen in figure 2(a), but alignment uniformity would likely benefit from application of a negative substrate bias during PECVD synthesis [17]. Despite obtaining a length exceeding several microns, CNTs and small CNT

bundles maintain a vertical orientation or form vertically oriented loops. Additional horizontally oriented CNTs are observed on the top PAA surface (figures 2(b)–(c)). We note that the cross-sectional FESEM images were obtained by cleaving the PAA, thereby releasing the CNTs from their pores of origin. As such, identifying the origin of CNTs within the pores using cross-sectional images is difficult, although one such image is shown in figure 2(d). Numerous CNTs may be observed emerging from their pores of origin, however, by examining the top PAA surface, as seen in figure 2(b).

CNT density was not a strong function of starting catalyst film thickness for iron layers between 1 and 10 nm for the synthesis conditions previously mentioned. Density was affected by altering the distance from the PAA top surface to the catalyst layer. A catalyst layer embedded further from the top PAA surface resulted in lower density. Similar findings have been reported for MWNT synthesis from PAA pores using PECVD [13]. Delamination of the film at the Al/Fe/Al interface often occurred when anodizing films with Fe layers greater than 10 nm.

HRTEM images, such as those in figures 3(a) and (b), reveal a mixture of SWNTs and DWNTs produced from the modified PAA structure. The observed average diameter of both SWNTs and DWNTs based on HRTEM was approximately 2 nm. Micro-Raman spectroscopy using a 785 nm excitation wavelength and 50× magnification was also used to characterize the CNT yield. Peaks at 132, 202, and 302

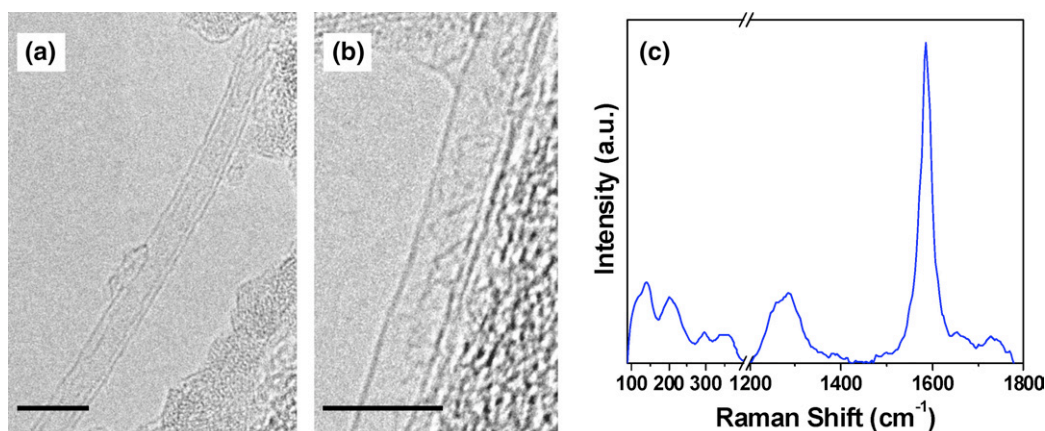


Figure 3. HRTEM image of a (a) DWNT and (b) SWNT. (c) Raman spectrum of CNTs grown from nanoporous alumina template with 1 nm Fe layer. Scale bar = 5 nm.

(This figure is in colour only in the electronic version)

wavenumbers correspond to radial breathing modes (RBMs), while peaks near 1300 and 1580 cm^{-1} indicate disordered and graphitic carbon (D- and G-bands), respectively. The diameter of SWNTs may be determined using the relation $d = 248/w_{\text{RBM}}$, where d is the diameter in nm, and w_{RBM} is the position of the RBM peak in cm^{-1} [28]. The relation may also be used to approximate the diameter of inner and outer shells of DWNTs. The RBM peaks observed thus correspond to SWNT diameters and/or shells of DWNTs of 1.9, 1.2, and 0.8 nm, respectively, in agreement with HRTEM analysis. In addition, the intensity ratio of the G-band to D-band, a metric for SWNT quality, is approximately 4, indicating relatively high-quality CNTs. The broadening and intensity of the D-band may originate from contributions of amorphous carbon deposited on the pore walls.

4. Conclusions

A PAA template with a localized catalyst layer embedded into the pore walls has been used for the first time to synthesize CNTs. HRTEM and Raman spectroscopy reveal that a mixture of SWNT and DWNTs are synthesized, while FESEM reveals CNTs initiating from the catalyst layer and emerging from their pores of origin. Fe was found to be the most suitable for integration into the structure, as it yielded the highest CNT density and greatest structural integrity. The structure contains a conductive Ti layer underneath the PAA template to serve as the anode for future electrodeposition of nanowires to electrically address the bottom surface of the CNTs. Further processing and optimization of the structure is expected to enable densely packed CNT-based electronic and sensing devices by functionalization of the CNTs within the vertical pores.

Acknowledgments

The authors would like to thank Professor Joseph Irudayaraj for access to the Raman instrument and gratefully acknowledge funding from the NASA-Purdue Institute for Nanoelectronics

and Computing and the Birck Nanotechnology Center in support of this work.

References

- [1] Avouris P, Appenzeller J, Martel R and Wind S J 2003 *Proc. IEEE* **91** 1772
- [2] Saito R, Dresselhaus G and Dresselhaus M S 1999 *Physical Properties of Carbon Nanotubes* (London: Imperial College Press)
- [3] Bachtold A, Fuhrer M S, Plyasunov S, Forero M, Anderson E H, Zettl A and McEuen P L 2000 *Phys. Rev. Lett.* **84** 6082
- [4] Shimada T, Sugai T, Ohno Y, Kishimoto S, Mizutani T, Yoshida H, Okzaki T and Shinohara H 2004 *Appl. Phys. Lett.* **84** 2412
- [5] Javey A, Kim H, Brink M, Wang Q, Ural A, Guo J, Mcintyre P, McEuen P, Lundstrom M and Dai H 2002 *Nat. Mater.* **1** 241
- [6] Li J, Zhang Q, Yang D and Tian J 2004 *Carbon* **42** 2263
- [7] Peng H, Ristorph T G, Schurmann G M, King G M, Yoon J, Narayanamurti V and Colovchenko J A 2003 *Appl. Phys. Lett.* **83** 4238
- [8] Javey A, Tu R, Farmer D, Guo J, Gordon R and Dai H 2005 *Nano Lett.* **5** 345
- [9] Che G, Lakshmi B B, Martin C R and Fisher E R 1998 *Chem. Mater.* **10** 260
- [10] Li J, Papadopoulos C and Xu J M 1999 *Appl. Phys. Lett.* **75** 367
- [11] Suh J S and Lee J S 1999 *Appl. Phys. Lett.* **75** 2047
- [12] Jeong S-H, Hwang H Y, Hwang S-K and Lee K-H 2004 *Carbon* **42** 2073
- [13] Yen J-H, Leu I-C, Wu M T, Lin C-C and Hon M-H 2004 *ElectroChem. Solid-State Lett.* **7** H29
- [14] Choi W B, Cheong B-H, Kim J J, Chu J and Bae E 2003 *Adv. Funct. Mater.* **13** 80
- [15] Xu T T, Fisher F T, Brinson L C and Ruoff R S 2003 *Nano Lett.* **3** 1135
- [16] Yanagishita T, Sasaki M, Nishio K and Masuda H 2004 *Adv. Mater.* **16** 429
- [17] Maschmann M R, Amama P B, Goyal A, Iqbal Z and Fisher T S 2006 *Carbon* at press
- [18] Masuda H and Satoh M 1996 *Japan. J. Appl. Phys.* **35** L126
- [19] Rabin O, Herz P R, Lin Y-M, Akinwande A I, Cronin S B and Dresselhaus M S 2003 *Adv. Funct. Mater.* **13** 631
- [20] Tian M, Xu S, Wang J, Kumar N, Wertz E, Li Q, Campbell P, Chan M H W and Mallouk T E 2005 *Nano Lett.* **5** 697

- [21] Franklin A D, Maschmann M R, Dasilva M, Janes D B, Fisher T S and Sands T D 2006 *Small* in review
- [22] Hata K, Futaba D N, Mizuno K, Namai T, Yumura M and Iijima S 2004 *Science* **306** 1362
- [23] Hornyak G L, Grigorian L, Dillon A C, Parilla P A, Jones K M and Heben M J 2002 *J. Phys. Chem. B* **106** 2821
- [24] Kong J, Soh H T, Cassell A M, Quate C F and Dai H 1998 *Nature* **395** 878
- [25] Kong J, Cassell A M and Dai H 1998 *Chem. Phys. Lett.* **292** 567
- [26] Hafner J H, Bronikowski M J, Azamian B R, Nikolaev P, Rinzler A G, Colbert D T, Smith K A and Smalley R E 1998 *Chem. Phys. Lett.* **296** 195
- [27] Maschmann M R, Amama P B, Goyal A, Iqbal Z, Gat R and Fisher T S 2006 *Carbon* **44** 10
- [28] Dresselhaus M S, Jorio A, Souza Filho A G, Dresselhaus G and Saito R 2002 *Physica B* **323** 15